IEEE Access
Multidisciplinary | Rapid Review | Open Access Journal

IEEE Power & Energy Society Section

Received 15 May 2024, accepted 26 June 2024, date of publication 10 July 2024, date of current version 31 July 2024.

*Digital Object Identifier 10.1109/ACCESS.2024.3425911*

RESEARCH ARTICLE

# High-Speed Rail Electric Traction Carbon Emission Calculation Method Based on Carbon Flow Theory

**SONG JINWEI[1], CHEN XIANG[1], LU CAIXIA[2], SHI XIN[1], YAN YUE[1], AND ZHANG SHIZE[1]**

[1]Big Data Center of State Grid Corporation of China, Beijing 100031, China
[2]Beijing Guodian Tong Network Technology Company Ltd., Beijing 100085, China

Corresponding author: Song Jinwei (ysjk2000@qq.com)

This work was supported in part by the Big Data Center Technology Project of State Grid Corporation of China under Contract SGSJ0000NYJS2310072.

**ABSTRACT** With global warming and escalating environmental pressures, low-carbon development has become a consensus. Against this backdrop, this study proposes an innovative method for calculating the carbon emissions from electric traction of high-speed trains. Utilizing reverse power flow tracing technology, the method precisely determines the supply structure of high-speed railway traction stations, where the carbon emission factors of electricity vary at different times and locations due to changes in power grid dispatching and supply mix. This approach facilitates the construction of a finely-tuned dynamic model of carbon emission factors at the provincial, municipal, and traction station levels to calculate the carbon emissions from high-speed railway electric traction. Based on this model, the study conducts time-segmented calculations of carbon emissions, comprehensively capturing the dynamics of carbon emissions during the electric traction process of high-speed railways. A lateral comparison with traditional modes of travel, such as cars and airplanes, reveals that high-speed railways have a significant advantage in terms of per capita carbon emissions, furthering the scientific basis for promoting high-speed railways as a green mode of travel. In fact, empirical analysis results show that this method can accurately quantify the carbon emissions during the electric traction phase of high-speed railway operations, providing decision support for train operators to optimize their operational strategies, and offering passengers reference information for making more environmentally-friendly travel choices.

**INDEX TERMS** Low-carbon development, reverse power flow tracing technology, dynamic electricity carbon emission factors, electric train traction carbon emissions, green travel.

## I. INTRODUCTION

In September 2020, President Xi Jinping announced at the 75th session of the United Nations General Assembly that ''China will enhance its nationally determined contributions, adopt more vigorous policies and measures, and aim to peak carbon dioxide emissions before 2030 and achieve carbon neutrality before 2060'' [1]. According to data from the International Energy Agency, the total global carbon emissions from fossil energy exceeded 37 billion tons in 2021 [2], [3], and from a sectoral perspective, the transportation sector accounts for roughly 16.2%-25% of global carbon emissions [4]. Studies have indicated that the carbon emissions from China's transportation sector account for approximately 7.6%-11% of the country's total emissions [5], [6], [7]. High-speed rail (hereinafter referred to as ''HSR''), as a fast, efficient, and eco-friendly mode of transportation, has significant advantages in reducing carbon emissions and improving transportation efficiency. Research on HSR carbon emissions helps to promote low-carbon development planning in China's transportation industry.

Domestic and international scholars have generally categorized the calculation of high-speed rail carbon emissions into two types: one adopts the construction of models using

The associate editor coordinating the review of this manuscript and approving it for publication was Maria Carmen Falvo.

carbon emission factors, or calculates the carbon emissions of the entire train journey based on the life cycle theory of train operation; the other constructs segmented models to calculate carbon emissions at each stage. Reference [8] conducted a study on the CO2 emissions of China's transportation industry and various modes of transportation including high-speed rail, analyzing and comparing the carbon emission structure of China's transportation industry and the carbon emission intensity of different modes of transportation, with high-speed rail emissions being relatively low. Reference [9] examined motor vehicles within urban transportation modes, where a calculation model for carbon dioxide emissions from rail transit was established, which can be expanded to high-speed rail. Investigated the energy consumption patterns, mode energy efficiency, and carbon dioxide emissions of private and public transport in 84 cities worldwide; their survey results can provide guidance for our research on the energy consumption and emissions of high-speed rail. Reference [10] conducted a preliminary analysis of the urban transportation characteristics, energy use, and greenhouse gas emissions of different cities in China. Reference [11] compiled high-speed rail energy consumption from aspects such as mileage and traction methods, comparing carbon emissions of transportation modes such as airplanes and high-speed rail, with high-speed rail being the lowest. Reference [12] suggests that the opening of high-speed rail significantly reduces the carbon emission intensity of cities along its route, with regional heterogeneity, with its carbon reduction effects being notable in cities in central and western China. Reference [13] argues that the opening of high-speed rail not only reduces carbon emissions in that city but also reduces those of neighboring cities through spatial technological spillover effects. Reference [14] compared the carbon emissions of electric locomotives versus fuel locomotives, concluding that electric traction offers a clear reduction in emissions. A series of studies have conducted life cycle assessments on high-speed rail carbon emissions. References [15], [16], [17] view that most railway system emissions come from the construction phase, due to the use of large quantities of construction materials and high-energy construction machinery, followed by the operational phase; Reference [18] considers that the operation and maintenance phase has the most significant emissions; Reference [16] created an environmental life cycle assessment to evaluate automobile, heavy rail, and aviation transport, highlighting that high-speed rail could reduce energy consumption and greenhouse gas emissions per trip, but may produce more sulfur dioxide emissions. Reference [19] compared high-speed rail's energy use and pollution emissions within a life cycle framework, discovering that carbon emissions and energy consumption are primarily from the construction, operation and maintenance phases. References [20], [21], and [22], all based on Reference [23], propose a calculation model based on traction work. The energy consumption of each train section is calculated by determining the distance and average speed between platforms.

In summary, current research mainly focuses on calculating the total line-route carbon emissions of trains, using international unified carbon emission factors when calculating carbon emissions. However, there is still a research gap regarding the calculation of train carbon emissions for individual operating segments, with only a few scholars studying train energy consumption per segment. Moreover, the precision of high-speed rail (HSR) carbon emission calculations is low, which is increasingly not meeting the requirements for accurate carbon accounting and is not conducive to low-carbon development and planning in the transportation sector. The primary electricity consumption in HSR operation comes from locomotive traction, and the proportion of clean energy in the electricity directly relates to carbon emissions from the power system. China's power energy structure is still mainly based on fossil fuels as the primary source of electricity generation, resulting in relatively high indirect carbon emission coefficients [24], [25]. Since HSR operations depend on the electricity system, this paper combines the ''carbon emission flow'' theory of the power system [26], [27], [28] and proposes a method for calculating HSR electric traction carbon emissions based on dynamic electricity emission factors. By constructing a reverse grid power flow tracing method and dynamic electric power emission factor calculation method, we calculate carbon emissions for an entire train journey and for each operational segment of every trip.

This paper makes three primary contributions:

1)Proposing a reverse tracing method based on the existing ''carbon flow theory'' and applying this method to calculate the power carbon emission factors of HSR electricity traction stations, which saves calculation time for carbon flows.

2)Proposing methods for calculating power traction carbon emissions for HSR segments, train traction carbon emissions, and per capita traction carbon emissions, realizing accurate calculation of HSR traction carbon emissions from different perspectives.

3)Utilizing the advantages of electric power big data, this paper integrates electric power big data with transportation data and validates the model with real data, laying the foundation for future research.

This paper firstly introduces the overall calculation method, then separately presents the method for calculating power carbon emission factors for HSR based on the improved carbon flow model, the methods for calculating HSR segment, train, and per capita electric traction carbon emissions, and finally validates the model using data from an actual HSR line.

## II. HIGH-SPEED RAIL ELECTRIC TRACTION CARBON EMISSION CALCULATION MODEL

### A. MODEL OVERVIEW

This paper presents a calculation model for carbon emissions generated by electric traction during the operation of high-speed rail, which is mainly produced by the electricity driving

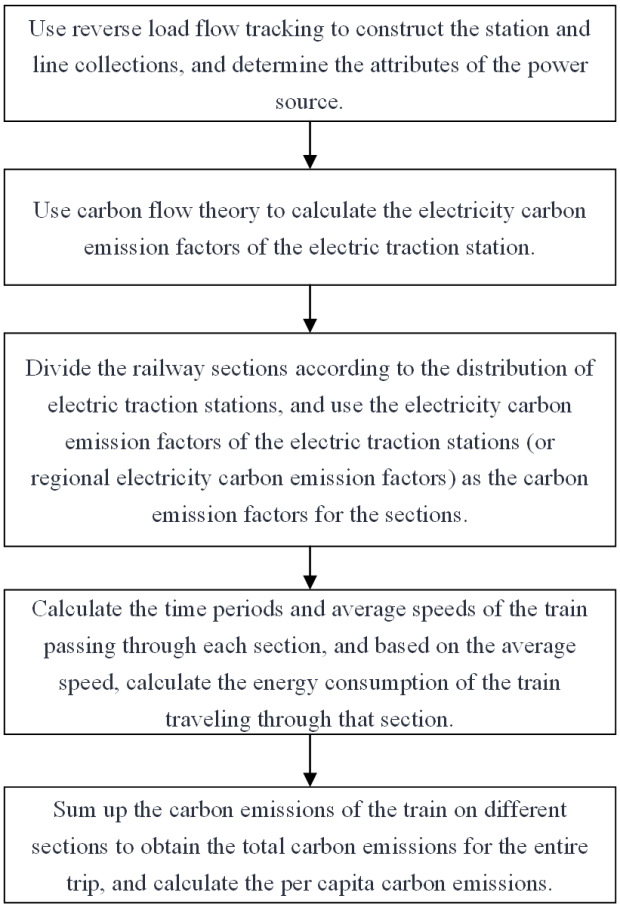


**FIGURE 1.** Algorithm overall flowchart.

the high-speed trains, called indirect carbon emission. This electricity primarily comes from electric traction stations along the high-speed rail line. The overall thinking of this method is to trace the power sources of the high-speed rail's electric traction stations in the power grid system to calculate their electricity carbon emission factors. Then, the carbon emissions are calculated based on the power consumption and the duration of the high-speed rail operation, as well as the distance traveled. The overall process of this method is shown in Figure 1.

In this method, the key of the carbon emission factor calculation is the electric traction stations. In this step, the "carbon flow theory" is adopted. By calculating the electricity carbon emission factor of electric traction stations, the calculation can be precise to hourly level under the condition of sufficient data. For certain sections where data is not obtainable, it is suggested to use the electricity carbon emission factor of the city's electric traction station. If a city-level factor is not available, then a provincial-level or even a national electricity carbon emission factor can be used as a substitute. Clearly, using a larger regional electricity carbon emission factor cannot guarantee the accuracy of the calculation. Currently, provincial electricity carbon emission factors can be calculated monthly through data from the power grid companies, while national factors are issued annually by the Ministry of Ecology and Environment, using for the calculation of indirect carbon emissions in the carbon market. As for high-speed rail, the duration of a single trip rarely exceeds 24 hours, using carbon emission factors with coarser granularity may lead to an error of 10% to 30% [27].

### B. CONSTRUCTION OF STATION AND ROUTE COLLECTION

References [28], [29] provide the basic model and definition of carbon flow. The main principle of carbon flow theory is using the adjacency property in the calculation of node carbon potentials. By consecutively querying nodes with unknown carbon potential and through several iterations of recursion, the carbon potential of all nodes in the system can be determined, which then reveals the distribution of carbon emission flows. This method requires the information of all plants and lines in the region, and construct the power grid topology graph. Trace forward from the power plant to track the carbon emissions transmitted with the current to the user. To calculate the electricity carbon emission factor for high-speed rail sections, it is only necessary to know the carbon emission factor of the electric traction stations, without the need to acquire information of all the plants on the railway passing line. According to "carbon flow theory," the electric power carbon emission factor of each station is related to the active input of the connected unit and other stations, but not related to the active output. Therefore, in the calculation process, one can utilize the natural directed graph characteristics of the power grid and employ reverse graph search algorithms to obtain the plants that can affect the carbon emission factor of the electric traction stations. This method simplifies the algorithm, allowing to use both depth-first and breadth-first search algorithms. As shown in Figure 2, this paper adopts the reverse tracking approach to track the plants with a power supply relationship to the electric traction stations and builds the related plant collection.

The search algorithm makes the electric traction station $s_1$ as the starting point $S = \{s_1\}$ and performs reverse load flow track, which is a backward search. Taking a depth-first search as an example, following the direction of the input power, the algorithm retrieves the next plant node. If this node $S$ already exists in the set, it indicates that there is a loop in the search process, then stop searching and backtrack to the previous node, and change the input line route for the reverse search. If the node $S$ does not exist in the set, it is added to $S$. If the node has no input lines, it indicates that it is a power generation plant. The algorithm then backtracks to the previous node and changes the input line route for reverse searching. Otherwise, the algorithm selects one input line to continue the search for the next node. The specific search details are as follows:

The search process is illustrated in Figure 3.

After completing the construction of the station node collection $S$, the set of lines $L$ should be constructed, meaning all lines connected to every power grid node within $S$ should be added to $L$. Using $S$ and $L$, a directed graph of the power grid that affects the electric traction stations can be built, where the

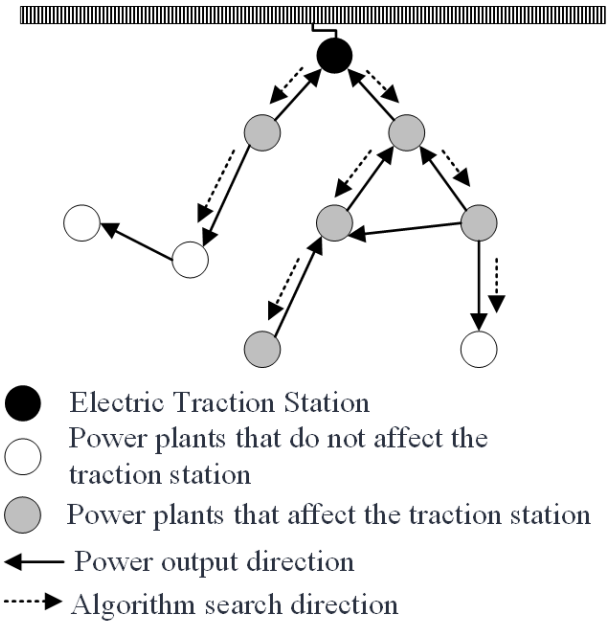


**FIGURE 2.** Schematic diagram of reverse searching.

**Algorithm 1** Reverse Load Flow Tracking

Input: Node $T$ representing the electric traction station as the starting point

Output: The traced path $P$ from electric traction station $T$

```
Initialize an empty set named searched
Initialize an empty stack named stack
Push the node traction_station onto stack
while stack is not empty do
    current ← top element of stack
    if current is not in searched then
        Add current to searched
        next_nodes ← GetAllInputNodes(current)
        if next_nodes is empty then
            Pop the top element from stack
        else
            for each node next in next_nodes do
                if next is not in searched then
                Push next onto stack
        else
            Pop the top element from stack
    Convert searched into a list named Path
    return Path
```

weight of the edges in the graph represents the active power on the lines.

For power plants in the collection $S$, clear attributes must be defined, specifically the type of generation units. Based on different categories of units, one should select the types of generating units connected to each plant and their corresponding power generation carbon emission factors $\varepsilon_m$, where $m$ representing the type of the generation unit. The electrical carbon emission factors could be derived from

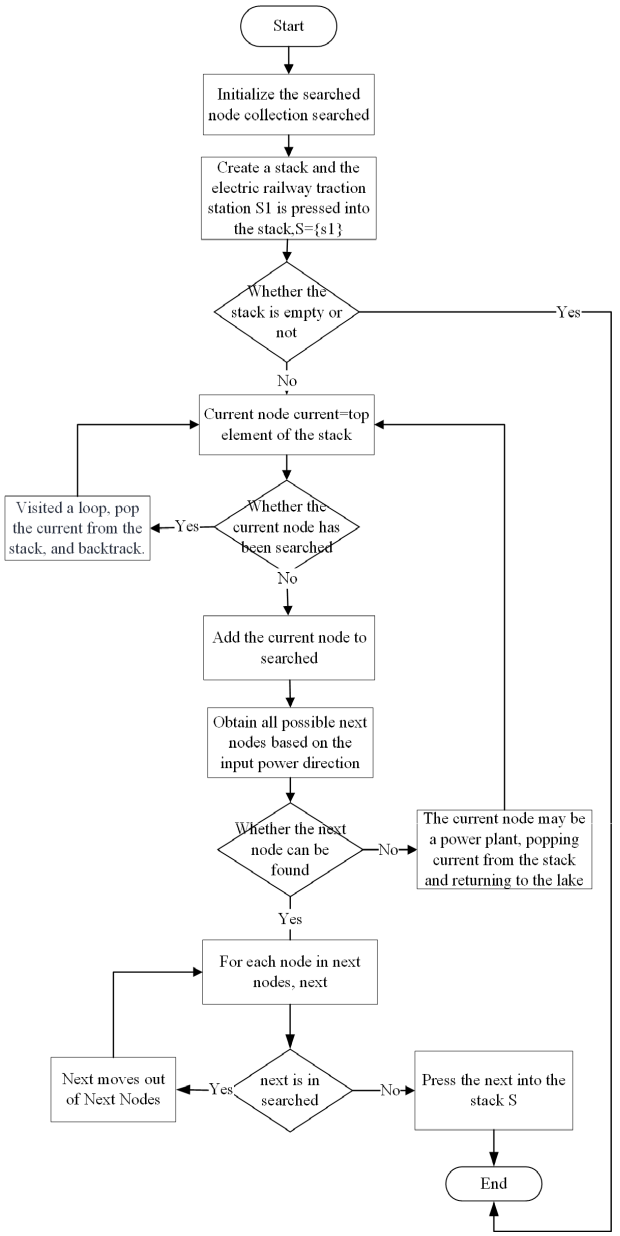


**FIGURE 3.** Reverse search process flowchart.

the IPCC's default power generation carbon emission factors [30], or from the unit carbon emission quota factors periodically released by the Ministry of Ecology and Environment [31]. A more accurate method is to calculate by the power plant data according to the power generation carbon emission calculation standards.

### C. CALCULATION OF ELECTRICITY CARBON EMISSION FACTORS FOR ELECTRIC TRACTION STATIONS

Based on the "carbon flow theory," carbon emissions from the generation side can be transmitted to the consumption side through the power grid's load flow. Taking a load flow section at a certain time t as an example, to calculate the electricity carbon emission factors for each node, it is necessary to establish a carbon flow balance equation for every power grid

statio.

$$C_i + \sum_j P_{j,i}\lambda_j = \left(E_i + \sum_j P_{j,i}\right)\lambda_i \tag{1}$$

In this equation, $E_i$ represents the electricity generated by the generating units connected to the node. If there are multiple types of units connected to the same node, and the generating electricity of each type of unit is $E_{i,m}$, then there appears $E_i = \sum_m E_{i,m}$. $C_i$ represents the carbon emissions produced by the electricity generation of the units connected to the node, which can be expressed as follows:

$$C_i = \sum_m E_{i,m}\varepsilon_m \tag{2}$$

Let $P_{j,i}$ represent the amount of electricity input from node $i$ to node $j$, then let $\lambda_i$ and $\lambda_j$ represent the electricity carbon emission factors of nodes $i$ and $j$ respectively. By combining the carbon flow balance equations of each node, we have the following system of equations:

$$\boldsymbol{M}\boldsymbol{\lambda} = \boldsymbol{C} \tag{3}$$

where the flow information matrix $\boldsymbol{M}$ is formed based on the collection $S$, $L$ and the power grid load flow, its composition is as follows:

$$\boldsymbol{M} = \boldsymbol{E} - \boldsymbol{P} + diag(\boldsymbol{P}\boldsymbol{\xi}) \tag{4}$$

where, if the number of elements in collection $S$ is $N$, then we have:

$$\boldsymbol{E} = \begin{bmatrix} E_1 & \cdots & 0 \\ \vdots & \ddots & \vdots \\ 0 & \cdots & E_N \end{bmatrix},$$

$$\boldsymbol{P} = \begin{bmatrix} 0 & P_{2,1} & \cdots & P_{N,1} \\ P_{1,2} & 0 & \vdots & P_{N,2} \\ \vdots & \vdots & \ddots & \vdots \\ P_{1,N} & P_{2,N} & \cdots & 0 \end{bmatrix},$$

$$\boldsymbol{\lambda} = [\lambda_1, \cdots, \lambda_N]^{\mathrm{T}}$$

as well as

$$\boldsymbol{C} = [C_1, \cdots, C_N]^{\mathrm{T}}.$$

Additionally, in the equation, $\boldsymbol{\xi}$ represents an $N$ dimensional column vector where all elements are 1. By using the formula to solve $\boldsymbol{\lambda}$, we have:

$$\boldsymbol{\lambda} = \boldsymbol{M}^{-1}\boldsymbol{C} \tag{5}$$

$\boldsymbol{\lambda}$ contains the electricity carbon emission factors of all the power stations in $S$. If we set the electric traction station as the first power station, then the carbon emission factor for that electric traction station can be represented as follows $\mu = \lambda_1$.

The above is an explanation for the load flow section of a single electric traction station at a specific time period $t$. If one were to calculate multiple sections, it would be necessary to add the subscript t to the following variables: If there are $K$ electric traction stations in the railway, this method can be used to determine the electricity carbon emission factors $\{\mu_{1,t}, \cdots, \mu_{K,t}\}$ for all traction stations at every moment $t$.

If the data for the province where the electric traction station is located does not support carbon flow calculation, it may be considered to use the provincial electricity carbon emission factor as a substitute. The method for calculating the provincial electricity carbon emission factor can follow the approach proposed in reference [32].

### D. SEGMENTATION OF HIGH-SPEED RAIL SECTIONS AND LABELLING OF SECTIONAL CARBON EMISSION FACTORS

High-speed rail sections are divided according to the range of electric power delivered by the electric traction stations, typically using an equal division method, as shown in Figure 4. If an electric traction station cannot calculate its electricity carbon emission factor due to missing data, a regional factor is used, such as the fourth electric traction station shown in Figure 4, which uses the provincial electricity carbon emission factor $\Lambda_B$ of Province B as the carbon emission factor for that section.

If a section spans multiple provinces, it is still labeled according to the electricity carbon emission factor of the electric traction station supplying power to the section. If the electricity consumption of the section supplied by the $k$-th electric traction station during the time period $t$ is $E_{k,t}$, which can be obtained from the load data of the electric traction station, then the carbon emissions generated by the electricity of this section at this moment would be:

$$Cr_{k,t} = E_{k,t}\mu_{k,t} \tag{6}$$

By summing up the carbon emissions of all sections, the total carbon emissions for the entire route at time $t$ can be obtained. This article focuses on the electricity carbon emissions associated with train services, where the carbon emissions generated by a train service are related to the energy consumption of the train; in turn, the train's energy consumption is related to its speed and the duration of operation.

### E. SEGMENTATION OF HIGH-SPEED TRAIN ENERGY CONSUMPTION CALCULATION

Using the aforementioned factors, the carbon emissions of the train can be calculated according to the sections divided by the electric traction stations. The sections are determined based on the electric traction stations, and the train's average velocity is estimated according to the train timetable. From the average velocity, the power consumption of the high-speed train on that section can be calculated. Depending on the frequency of collection of the load flow sections, the electricity carbon emission factors for each section will vary over time, with updates that can be as frequent as every 15 minutes. This paper uses hourly-level electricity carbon emission factors. By multiplying the section's factor by the energy consumption of the train during its operation on the section, the carbon emissions can be obtained.

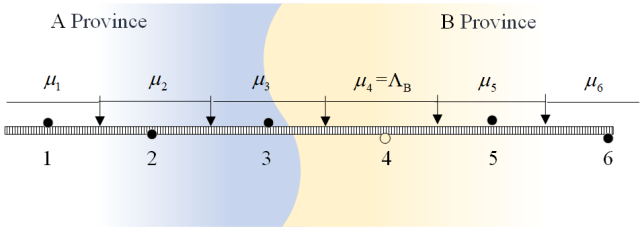


**FIGURE 4.** Schematic illustration of carbon emission factor labeling for high-speed rail sections.

Reference [33] provides different equations for train energy consumption and suggests that energy consumption during the traction phase is directly proportional to the square of the velocity. This paper calculates energy consumption by segmenting the route, converting the general equation into an equation for energy consumption for each segment, as shown in the below equation. In this equation, $w_{r,p,q}$ represents the energy consumption per ton per kilometer for train service $r$ on the segment between stations $p$ and $q$, with the unit being $KJ/t \cdot km^{-1}$. $v_{r,p,q}$ represents the average velocity of the train on the segment, and $L_{p,q}$ represents the distance between $p$ and $q$. The parameters $\alpha$ and $\beta$ need to be determined through fitting.

$$w_{r,p,q} = \alpha \frac{v_{r,p,q}^2}{\ln(L_{p,q})} + \beta \tag{7}$$

Based on the train timetable provided by the 12306 app, the average running speed of the train on each segment is calculated. The model of the train commonly used on the railway line studied in this article is predominantly CRH5. Typically, the passenger load of high-speed trains accounts for about 10% of the train's own weight [34]. With the CRH5 having a tare weight of 500 tons and a full load weight of 550 tons, the energy consumption $w_{r,p,q}$ is converted into electricity consumption $E_{r,p,q}$ by the following formula.

$$E_{r,p,q} = \theta w_{r,p,q} M_r L_{p,q} \tag{8}$$

where $M$ is the weight of the train after passenger load, and $\theta$ is the conversion factor from kilo-joules to megawatt-hours, with a value of 2.777778e-7. Usually, the distance between stations $p$ and $q$ is considerable, requiring multiple electric traction stations for power supply. If the length of the power supply section provided by each electric traction station is $l_k$, then the energy consumption of the train passing through each jurisdictional section is given by the following equation.

$$q_{r,k} = \frac{l_k}{L_{p,q}} E_{r,p,q} \tag{9}$$

For the railway sections under the jurisdiction of the electric traction stations at train stations $p$ and $q$, it is only necessary to calculate the range of the supplied sections between the stations.

### F. CALCULATION OF HIGH-SPEED TRAIN SERVICES AND PER CAPITA CARBON EMISSIONS

The carbon emission factor for the power-supply section of the electric traction station is consistent with the carbon emission factor of the electric traction station itself. The carbon emissions for the section equal the section's carbon emission factor multiplied by the high-speed train's electricity consumption. Suppose the k-th electric traction station of the railway line is responsible for section $l_k$; then the carbon emissions $cl_{r,t,k}$ due to traction of train service $r$ on this section during period $t$ is as follows:

$$cl_{r,k} = \mu_{t,k} q_{r,k} \tag{10}$$

The supply range of the electric traction station typically spans 40-50 km. For hourly carbon emission factors, based on the speed of the high-speed train, the carbon emission factor at the moment when the train enters the section can be selected for calculation. Usually, when the train service $r$ is determined, the time for each section can be estimated according to the train timetable, hence the subscript $t$ can be omitted.

Based on the above equation (10), calculating the traction carbon emissions of the train for a certain period and on a certain section. By summing the carbon emissions from the power supply sections of each electric traction station, the total traction-generated carbon emissions of train $r$ during its operation on that route can be obtained:

$$cl_r = \sum_{0}^{k} cl_{r,k} \tag{11}$$

This paper calculates the per capita carbon emissions $\overline{cl}_r$ of the high-speed train by dividing the train's carbon emissions by the number of full-load passengers $n_r$. The data on the full passenger capacity is obtained from the 12306 ticketing system.

$$\overline{cl}_r = \frac{cl_r}{n_r} \tag{12}$$

## III. EMPIRICAL ANALYSIS

### A. CALCULATION OF CARBON EMISSIONS FROM A HIGH-SPEED RAIL ELECTRIC TRACTION STATION IN NORTH CHINA

Taking the JZ high-speed rail line in North China as an example, the JZ high-speed rail route is powered by 6 traction stations, namely BJB,QH, BDLX, XBA, XBY, and ZJKN electric traction stations. The total distance of the route is 174km, with an approximate running time of 1.05 hours. The distances between sections are $l_{\mathrm{QH}}$,……, $l_{\mathrm{ZJKN}}$. By applying the reverse load flow tracking method, the related power plants are identified and incorporated along with the power grid's active load flow data and the electricity carbon emission factors calculated by the model, to compute the carbon emissions of the electric traction stations. The coefficients for calculating the energy consumption of each train operation stage are based on the fitted coefficients when the station

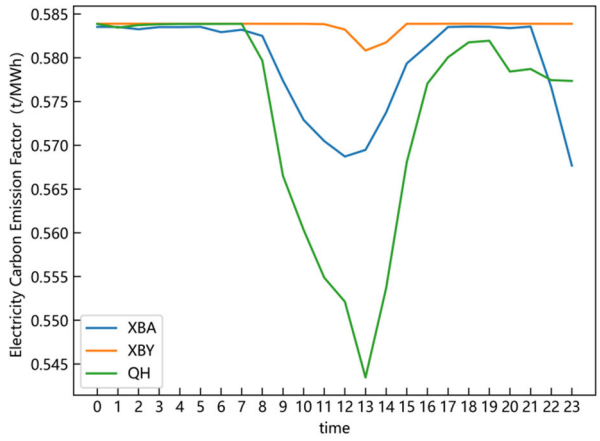


**FIGURE 5.** Diagram illustrating 24-hour carbon factor variation of traction stations.

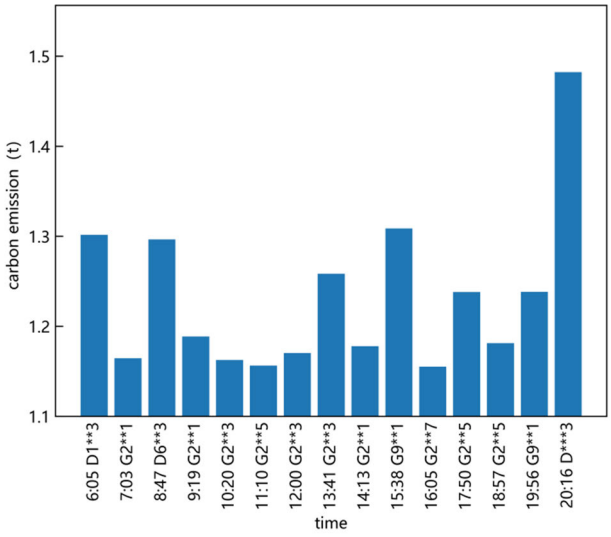


**FIGURE 6.** Diagram illustrating changes in train carbon emissions between 6 AM and 8 PM.

distance $l_k$ is less than 100 km as given in [35], with $\alpha = -0.00582$ and $\beta = 119.862$.

Figure 5 shows the 24-hour variation trend of the electricity carbon emission factors for the XBA, XBY, and QH traction stations. According to the data in the figure, it can be observed that from 8 to 17 o'clock, due to the significant output from wind and solar energy during these hours, the electricity carbon emission factors noticeably decrease.

The JZ high-speed rail runs its first and last trains of the day at 06:05 and 20:58 respectively. Figure 6 displays the carbon emissions corresponding to each train at different operating times. The results show that the carbon emissions produced by trains at different times vary, and traveling by train can be chosen based on the carbon emissions at different times.

Selecting six trains from different time periods, Table 1 provides detailed insight into basic information of each train such as model type, passenger capacity, departure time, sections traveled, and supplying traction stations, as well as calculated data including detailed carbon emissions by

**TABLE 1.** Comparison of high-speed rail carbon emissions at different times and sections.

| Train | Model | Passenger Capacity (people) | Departure Time | Train Carbon Emissions (t) | per capita carbon emissions (kg) |
|---|---|---|---|---|---|
| D1**3 | CRH5A | 586 | 6:05 | 1.301653 | 2.221250 |
| G2**3 | CR400BF-G | 576 | 12:00 | 1.170409 | 2.03196 |
| G2**1 | CR400BF-G | 576 | 13:41 | 1.25838 | 2.184686 |
| G2**7 | CR400BF-G | 576 | 16:05 | 1.155281 | 2.005696 |
| G2**5 | CR400BF-G | 576 | 18:57 | 1.181297 | 2.050863 |
| D***3 | CRH5A | 586 | 20:16 | 1.4823 | 2.529526 |

**TABLE 2.** Direct train electricity consumption and carbon emissions.

| Train | Departure Time | Section | operating duration | Electricity Consumption (MWh) | Carbon Emissions (t) |
|---|---|---|---|---|---|
| G2**3 | 13:41 | BJB-ZJK | 0.95 | 2.17578 | 1.25838 |
| G2**5 | 17:50 | BJB-ZJK | 0.93 | 2.14069 | 1.23808 |

traction station, total carbon emissions per trip, and per capita carbon emissions per trip. The carbon emissions for the six trains are respectively 1.3017 t, 1.1704 t, 1.2584 t, 1.1553 t, 1.1813 t, and 1.4823 t. For trains G2**3 and G2**5, which have the same model type, full capacity, and stop at the same stations, the carbon emissions calculated for each traction station and the per capita carbon emissions differ due to variation in the carbon emission factors at different departure times, thereby demonstrating that the variations in carbon emissions between trains of the same model, following the same stopping pattern, at different times, are due to differences in the electric power carbon emission factors of the traction stations. Observing the other four trains' data, it is found that D1**3 and D***3 trains have relatively higher energy consumption compared to other trains. This difference is attributed to the fact that they stop at more stations and their traction station carbon factors are relatively higher compared to other trains. Therefore, the conclusion is drawn that in terms of the total carbon emissions for an entire train journey, once the impact of the high-speed train information itself is excluded, the main determinants in calculating high-speed train carbon emissions currently are the changes in train traveling speed and carbon emission factors.

The aforementioned conclusion is drawn from an analysis of the entire train journey. Next, an in-depth analysis of carbon emissions from each running section of the train and the main influencing factors of the emissions is conducted. First, all the trains within a day are classified by whether they have the same stopping stations, resulting in four categories: non-stop, one stopping station, two stopping stations, and

**TABLE 3.** One-stop train electricity consumption and carbon emissions.

| Train | Departure Time | Section | operating duration | Electricity Consumption (MWh) | Carbon Emissions (t) |
|---|---|---|---|---|---|
| G2**7 | 7:03 | BJB-QH | 0.2 | 0.18910 | 0.10986 |
| | | QH-ZJK | 0.8 | 1.80724 | 1.05467 |
| G2**1 | 9:19 | BJB-QH | 0.2 | 0.18910 | 0.10981 |
| | | QH-ZJK | 0.82 | 1.85334 | 1.07901 |
| G2**3 | 10:20 | BJB-QH | 0.2 | 0.18910 | 0.11002 |
| | | QH-ZJK | 0.8 | 1.80724 | 1.05264 |
| G2**5 | 11:10 | BJB-QH | 0.2 | 0.18910 | 0.10999 |
| | | QH-ZJK | 0.8 | 1.80724 | 1.04642 |
| G2**1 | 14:13 | BJB-QH | 0.2 | 0.18910 | 0.11028 |
| | | QH-ZJK | 0.82 | 1.85334 | 1.06774 |
| G2**7 | 16:05 | BJB-QH | 0.2 | 0.18910 | 0.10835 |
| | | QH-ZJK | 0.8 | 1.80724 | 1.04693 |

**TABLE 4.** Two-stop train electricity consumption and carbon emissions.

| Train | Departure Time | Section | operating duration | Electricity Consumption (MWh) | Carbon Emissions (t) |
|---|---|---|---|---|---|
| G2**3 | 12:00 | BJB-QH | 0.2 | 0.189096 | 0.10925 |
| | | QH-XHB | 0.7 | 1.554134 | 0.89760 |
| | | XHB-ZJK | 0.17 | 0.280763 | 0.16355 |
| G2**5 | 18:57 | BJB-QH | 0.2 | 0.189096 | 0.11035 |
| | | QH-XHB | 0.7 | 1.554134 | 0.90723 |
| | | XHB-ZJK | 0.17 | 0.280763 | 0.16371 |

multiple stopping stations, with the latter category referring to those trains with more than two stopping stations that all differ.

Table 2 shows the power consumption and carbon emissions of non-stop trains. Trains G2**3 and G2**5 have the same running distance, stopping stations, and model type, but different power consumption. The reason for this is that these trains have different operating durations, leading to variations in travel speed, which then results in different calculated carbon emissions.

Table 3 presents the electricity consumption and carbon emissions of trains with one intermediate stopping station for each segment of their journey. Trains G2**7, G2**3, G2**5, and G2**7 have the same traveling distances on the BJB-QH and QH-ZJK sections, the same operating durations for each segment, and the same train models, which results in identical calculated electricity consumptions. However, the carbon emissions of these four trains are all different. This is because each operational segment is powered by different

**TABLE 5.** Multi-stop trai electricity consumption and carbon emissions.

| Train | Departure Time | Section | operating duration | Electricity Consumption (MWh) | Carbon Emissions (t) |
|---|---|---|---|---|---|
| D1**3 | 6:05 | BJB-QH | 0.22 | 0.19092 | 0.10941 |
| | | QH-BDL | 0.37 | 0.66573 | 0.38870 |
| | | BDL-XHYB | 0.38 | 0.79407 | 0.46288 |
| | | XHYB-XHB | 0.17 | 0.30326 | 0.17692 |
| | | XHB-ZJK | 0.17 | 0.28076 | 0.16374 |
| D6**3 | 8:47 | BJB-QH | 0.20 | 0.18910 | 0.11041 |
| | | QH-BDL | 0.37 | 0.66573 | 0.38871 |
| | | BDL-HL | 0.25 | 0.48711 | 0.28442 |
| | | HL-XHB | 0.30 | 0.59887 | 0.34967 |
| | | XHB-ZJK | 0.17 | 0.28076 | 0.16331 |
| G9**1 | 15:38 | BJB-QH | 0.20 | 0.18910 | 0.11032 |
| | | QH-BDL | 0.32 | 0.61179 | 0.35720 |
| | | BDL-DHYB | 0.17 | 0.28719 | 0.28719 |
| | | DHYB-HL | 0.15 | 0.26435 | 0.26435 |
| | | HL-XHB | 0.30 | 0.59887 | 0.34781 |
| | | XHB-ZJK | 0.18 | 0.29560 | 0.17249 |
| G9**1 | 19:56 | BJB-QH | 0.20 | 0.18910 | 0.11040 |
| | | QH-XHYB | 0.60 | 1.31498 | 0.76762 |
| | | XHYB-XHB | 0.18 | 0.33644 | 0.19640 |
| | | XHB-ZJK | 0.17 | 0.28076 | 0.16388 |
| D***3 | 20:16 | BJB-QH | 0.20 | 0.18910 | 0.11041 |
| | | QH-HL | 0.55 | 1.15975 | 0.67702 |
| | | HL-XHYB | 0.20 | 0.36168 | 0.36168 |
| | | XHYB-XHB | 0.18 | 0.33644 | 0.31997 |
| | | XHB-ZJK | 0.16 | 0.28076 | 0.16391 |

traction stations, and each electric traction station has a different electric power carbon emission factor. The data for trains G2**5 and G2**1 in Table 4 also confirm this: when the train model, stopping stations, and operating durations for each section are the same, their power consumption remains the same, and the differences in carbon emissions are due to the varying electric power carbon emission factors at each traction station.

Table 5 shows the electricity consumption and carbon emissions for each segment of the journey for trains with multiple stopping stations. The data in the table indicates that the stopping stations differ among the five trains, but they all

**TABLE 6.** The electricity consumption of each traction station at different times.

| Departure Time | BDLX (MWh) | BJB (MWh) | QH (MWh) | XBA (MWh) | XBY (MWh) | ZJKN (MWh) |
|---|---|---|---|---|---|---|
| 6:05 | 0.6115 | 0.0868 | 0.4000 | 0.6647 | 0.3032 | 0.1685 |
| 7:03 | 0.5164 | 0.0860 | 0.3276 | 0.6511 | 0.2806 | 0.1347 |
| 8:47 | 0.6134 | 0.0860 | 0.3990 | 0.6539 | 0.3008 | 0.1685 |
| 9:19 | 0.5295 | 0.0860 | 0.3334 | 0.6677 | 0.2878 | 0.1381 |
| 10:20 | 0.5164 | 0.0860 | 0.3276 | 0.6511 | 0.2806 | 0.1347 |
| 11:10 | 0.5164 | 0.0860 | 0.3276 | 0.6511 | 0.2806 | 0.1347 |
| 12:00 | 0.5070 | 0.0860 | 0.3236 | 0.6393 | 0.2997 | 0.1685 |
| 13:41 | 0.5819 | 0.0632 | 0.3289 | 0.7337 | 0.3162 | 0.1518 |
| 14:13 | 0.5295 | 0.0860 | 0.3334 | 0.6677 | 0.2878 | 0.1381 |
| 15:38 | 0.6271 | 0.0860 | 0.3750 | 0.6747 | 0.3068 | 0.1774 |
| 16:05 | 0.5164 | 0.0860 | 0.3276 | 0.6511 | 0.2806 | 0.1347 |
| 17:50 | 0.5725 | 0.0622 | 0.3236 | 0.7219 | 0.3111 | 0.1494 |
| 18:57 | 0.5070 | 0.0860 | 0.3236 | 0.6393 | 0.2997 | 0.1685 |
| 19:56 | 0.8074 | 0.0860 | 0.3800 | 0.6321 | 0.3241 | 0.1685 |
| 20:16 | 0.6132 | 0.0860 | 0.3698 | 0.9781 | 0.3241 | 0.1685 |

include the BJB-QH section. In this section, when the operating duration is 0.20 hours, the electricity consumption is consistently 0.18910 MWh, and when the operating duration is 0.22 hours, the electricity consumption is 0.19092 MWh.

Tables 2-5 all confirm that when the train's tare weight, stopping stations, and operating duration are consistent, the main determinant of its carbon emissions is the electric power carbon emission factor of the traction stations. Therefore, accurate calculation of the electric power carbon emission factor is particularly important.

Figure 7 shows the proportion of carbon emissions in different segments for trains, indicating that the energy consumption shares are almost consistent across segments for trains that stop at the same stations, such as G2**7, G2**1 and G2**3, G2**5 trains. There are also variations in corresponding proportions for trains stopping at different stations, such as the D1**7 and D6**3 trains.

Next, we analyze the structure and trends of train power consumption and carbon emissions from the perspective of traction stations.

Table 6 shows the electric energy consumption of various trains at different stations. The electricity consumption at each traction station varies slightly, mainly because the train's electricity consumption is related to its own weight, running duration, and the number of stops it makes. For the trains departing at 7:03, 9:19, 10:20, 11:10, and 16:05, which all have the same stops, their electricity consumption is virtually the same. The difference in the 9:19 train from the other four is due to its different running duration.

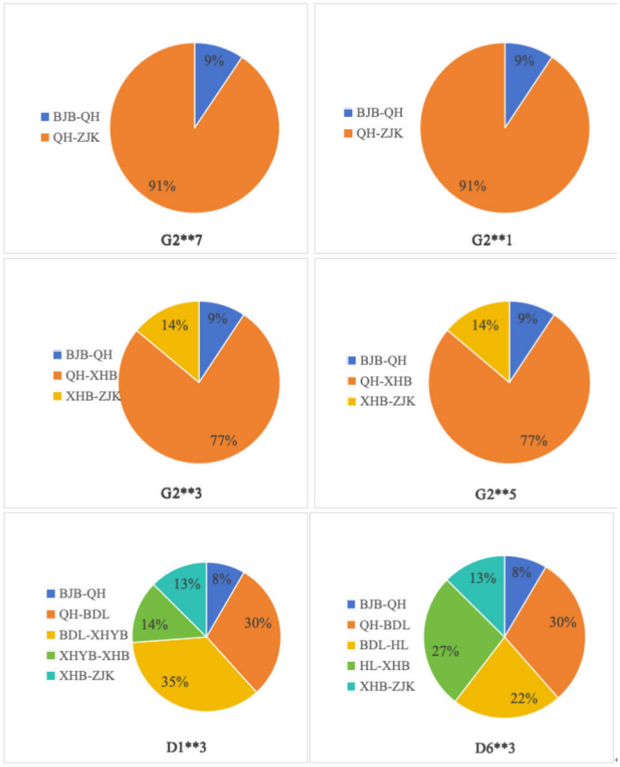


**FIGURE 7.** Carbon emission proportions for trains in each segment.

Figures 8 and 9 analyze the structure and trends of train carbon emissions from the perspective of traction stations. Figure 8 demonstrates the carbon emission share of each traction station at different departure times, while Figure 9 shows the carbon emissions of each traction station at these times. The results displayed in the figures indicate that due to different departure times, there is variability in the carbon emissions from the six traction stations. Figure 8 reveals a very stable ranking in the proportion of emissions from the six traction stations per journey, from largest to smallest: XBA, BDLX, QH, XBY, ZJKN, and BJB. The reason that BJB and ZJKN stations have the smallest carbon emissions is that these two stations act as the initiating and final supplying traction stations, respectively, with shorter supply distances. Figure 9 illustrates that there are differences in carbon emissions from the traction stations at different times, with BDLX, XBY, and ZJKN showing more noticeably fluctuating trends, due to changes in the proportion of coal-fired power supply and clean energy supply caused by power dispatch control.

### *B. COMPARISON WITH OTHER MODES OF TRANSPORTATION*

Currently, the main modes of transportation in the transport industry are rail, road, and air. High-speed rail, as an advanced mode of rail transport, is favored for its high speed, large transport capacity, and relatively low energy consumption. It is suitable for medium and long-distance transportation. Road transportation plays a crucial role in urban and rural transport with its point-to-point, flexible,

**TABLE 7. Per capita carbon emissions of different modes of transportation.**

| Mode of Transportation | | Speed/ (km • h$^{1}$ ) | Seating Capacity /people | Main Energy Source | Per Capita Carbon Emissions per 100 Kilometers/kg |
|---|---|---|---|---|---|
| Road, | small cars | 100 | 4 | Gasoline | 5.85 |
| | Passenger car | 90 | 19 | Diesel | 3.26 |
| Air | large airplanes | 800 | 300 | Aviation Kerosene | 8.05 |
| | Medium airplanes | 800 | 150 | Aviation Kerosene | 9.05 |
| | small airplanes | 800 | 50 | Aviation Kerosene | 12.07 |
| High-speed rail | D- | 200 | 600 | Electricity | 1.76 |
| | G- | 300 | 600 | Electricity | 1.85 |

Note: The data for road and air transportation modes in the table are sourced from reference [38], while the high-speed rail data are calculated using the algorithm proposed in this paper.

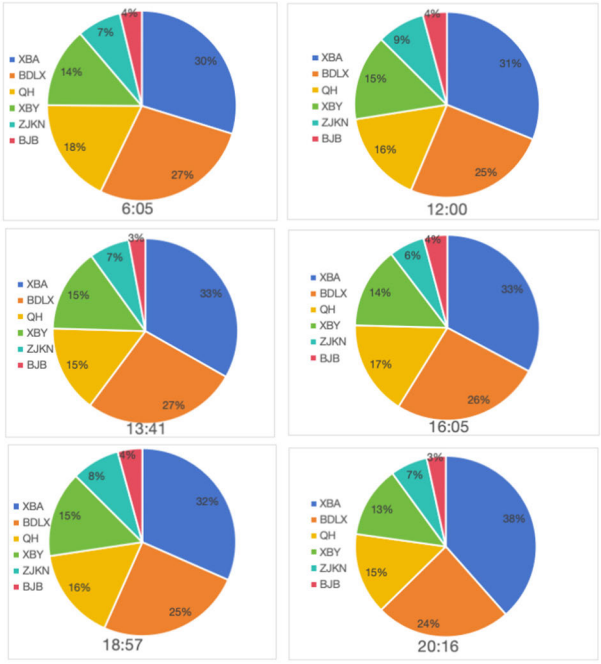


**FIGURE 8. Carbon emission proportions of traction stations in different time periods.**

and mobile characteristics, making it suitable for medium and short-distance transport. Air transportation is one of the fastest kinds of transport, capable of quickly covering long distances. This section will combine per capita carbon emission data for high-speed rail, road, and air transportation, focusing on the performance of each mode of transport in terms of environmental sustainability. The per capita carbon

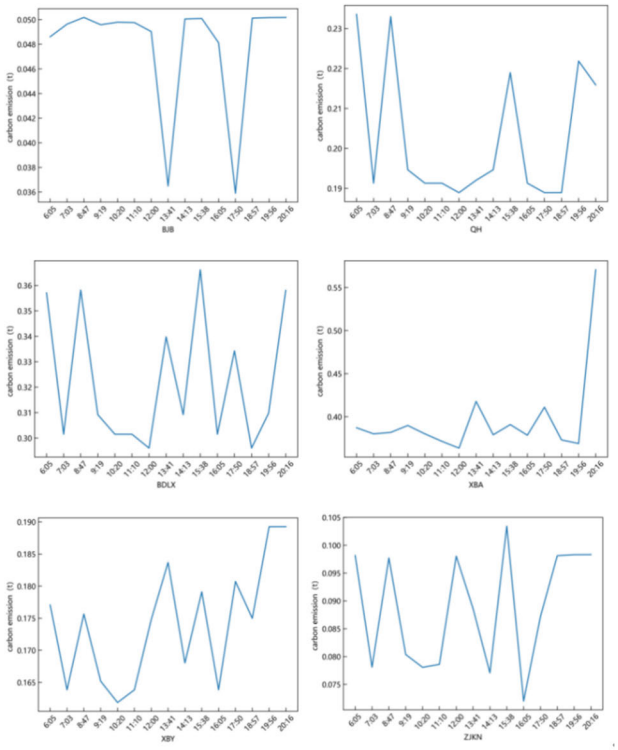


**FIGURE 9. Carbon emission trends of various traction stations.**

emissions for different modes of transport are shown in Table 3.

As shown in Table 7, high-speed rail transport is an efficient and energy-saving mode of travel. The carbon emissions from small cars are 3.32 times that of high-speed rail, from large airplanes are 4.57 times that of high-speed rail, and from small airplanes are 6.85 times that of high-speed rail. Overall, high-speed rail travel is more environmentally friendly with respect to carbon emissions when compared with road and air travel. Using high-speed rail can significantly reduce carbon emissions, making it a more sustainable travel option.

## IV. CONCLUSION

This paper proposes a method for calculating carbon emissions from high-speed rail electric traction based on dynamic electricity carbon emission factors. It employs the technology of reverse load flow tracing to determine the range for calculating carbon emissions from high-speed rail electric traction stations and introduces the concept of power supply time to calculate the dynamic carbon emission factors for provinces, cities, and traction stations. The aim is to accurately calculate the carbon emissions from high-speed rail electric traction and enable predictions of carbon emissions for each train service, providing a basis for choosing green travel options.

Through empirical analysis of the JZ railway line, this study shows that the use of dynamic electricity carbon emission factors can accurately calculate the carbon emissions produced by electric traction of high-speed trains. The results demonstrate that there are variations in carbon emissions across different electric traction stations, which suggests

**TABLE 8.** Table of train carbon emissions from 6 AM to 9 PM.

| Train | Model | Passenger Capacity (person) | Departure Time | Section | Supplying Traction Station | Electricity Consumption (MWh) | Electricity Carbon Emission Factor (t/MWh) | Carbon Emissions (t) | Train Carbon Emissions (t) | Per capita carbon emissions (kg) |
|---|---|---|---|---|---|---|---|---|---|---|
| D1**3 | CRH5A | 586 | 6:05 | BJB-QH | BJB | 0.086782399 | 0.560177176 | 0.048613519 | 1.301652721 | 2.221250378 |
| | | | | | QH | 0.104138879 | 0.583844786 | 0.060800941 | | |
| | | | | QH-BDL | QH | 0.295880952 | 0.583844786 | 0.172748551 | | |
| | | | | | BDLX | 0.36985119 | 0.583887482 | 0.21595148 | | |
| | | | | BDL-XHYB | BDLX | 0.241672578 | 0.583887482 | 0.141109593 | | |
| | | | | | XBA | 0.552394465 | 0.582497091 | 0.321768169 | | |
| | | | | XHYB-XHB | XBA | 0.112320188 | 0.582497091 | 0.065426183 | | |
| | | | | | XBY | 0.190944319 | 0.583886938 | 0.111489894 | | |
| | | | | XHB-ZJK | XBY | 0.112305367 | 0.583886938 | 0.065573637 | | |
| | | | | | ZJKN | 0.168458051 | 0.582760833 | 0.098170754 | | |
| G2**1 | CR400BF-G | 576 | 7:03 | BJB-QH | BJB | 0.085952736 | 0.577509155 | 0.049638492 | 1.164526968 | 2.021748208 |
| | | | | | QH | 0.103143283 | 0.583856525 | 0.060220879 | | |
| | | | | QH-ZJK | QH | 0.224502158 | 0.583856525 | 0.13107705 | | |
| | | | | | BDLX | 0.516354964 | 0.583888732 | 0.301493845 | | |
| | | | | | XBA | 0.651056259 | 0.58389558 | 0.380148872 | | |
| | | | | | XBY | 0.280627698 | 0.583855222 | 0.163845947 | | |
| | | | | | ZJKN | 0.134701295 | 0.57981539 | 0.078101884 | | |
| D6**3 | CRH5A | 586 | 8:47 | BJB-QH | BJB | 0.085952736 | 0.583888729 | 0.050186834 | 1.296522795 | 2.212496237 |
| | | | | | QH | 0.103143283 | 0.583874026 | 0.060222684 | | |
| | | | | QH-BDL | QH | 0.295880952 | 0.583874026 | 0.172757203 | | |
| | | | | | BDLX | 0.36985119 | 0.583890714 | 0.215952675 | | |
| | | | | BDL-HL | BDLX | 0.243556942 | 0.583890714 | 0.142210637 | | |
| | | | | | XBA | 0.243556942 | 0.58389558 | 0.142211822 | | |
| | | | | HL-XHB | XBA | 0.410334114 | 0.58389558 | 0.239592276 | | |
| | | | | | XBY | 0.18853189 | 0.583882648 | 0.110080499 | | |
| | | | | XHB-ZJK | XBY | 0.112305367 | 0.583882648 | 0.065573155 | | |
| | | | | | ZJKN | 0.168458051 | 0.580174171 | 0.09773501 | | |
| G2**1 | CR400BF-G | 576 | 9:19 | BJB-QH | BJB | 0.085952736 | 0.576941932 | 0.049589738 | 1.188815853 | 2.063916411 |
| | | | | | QH | 0.103143283 | 0.583847739 | 0.060219973 | | |
| | | | | QH-ZJK | QH | 0.230228547 | 0.583847739 | 0.134418416 | | |
| | | | | | BDLX | 0.529525657 | 0.583881284 | 0.30918012 | | |
| | | | | | XBA | 0.667662785 | 0.58389558 | 0.389845349 | | |
| | | | | | XBY | 0.287785683 | 0.573990996 | 0.165186391 | | |
| | | | | | ZJKN | 0.138137128 | 0.581855631 | 0.080375866 | | |

that carbon emission management should consider more detailed factors. This could guide users to choose more environmentally friendly and low-carbon travel options, furthering the development of green transportation.

**TABLE 8.** *(Continued.)* **Table of train carbon emissions from 6 AM to 9 PM.**

| | | | | | | | | | |
|---|---|---|---|---|---|---|---|---|---|
| G2**3 | CR400BF-G | 576 | 10:20 | BJB-QH | BJB | 0.085952736 | 0.579341933 | 0.049796024 | 1.162659872 | 2.018506722 |
| | | | | | QH | 0.103143283 | 0.583847617 | 0.06021996 | | |
| | | | | QH-ZJK | QH | 0.224502158 | 0.583847617 | 0.13107505 | | |
| | | | | | BDLX | 0.516354964 | 0.583881003 | 0.301489854 | | |
| | | | | | XBA | 0.651056259 | 0.58389558 | 0.380148872 | | |
| | | | | | XBY | 0.280627698 | 0.576795757 | 0.161864865 | | |
| | | | | | ZJKN | 0.134701295 | 0.579543398 | 0.078065246 | | |
| G2**5 | CR400BF-G | 576 | 11:10 | BJB-QH | BJB | 0.085952736 | 0.579021137 | 0.049768451 | 1.156408003 | 2.007652783 |
| | | | | | QH | 0.103143283 | 0.583837315 | 0.060218898 | | |
| | | | | QH-ZJK | QH | 0.224502158 | 0.583837315 | 0.131072737 | | |
| | | | | | BDLX | 0.516354964 | 0.583873896 | 0.301486184 | | |
| | | | | | XBA | 0.651056259 | 0.570486062 | 0.371418521 | | |
| | | | | | XBY | 0.280627698 | 0.583844417 | 0.163842914 | | |
| | | | | | ZJKN | 0.134701295 | 0.583515531 | 0.078600298 | | |
| G2**3 | CR400BF-G | 576 | 12:00 | BJB-QH | BJB | 0.085952736 | 0.570486062 | 0.049034838 | 1.170409116 | 2.031960271 |
| | | | | | QH | 0.103143283 | 0.583823924 | 0.060217516 | | |
| | | | | QH-XHB | QH | 0.220444545 | 0.583823924 | 0.128700799 | | |
| | | | | | BDLX | 0.507022454 | 0.583885641 | 0.29604313 | | |
| | | | | | XBA | 0.639289181 | 0.568719054 | 0.363575938 | | |
| | | | | | XBY | 0.187377863 | 0.58322851 | 0.109284112 | | |
| | | | | XHB-ZJK | XBY | 0.112305367 | 0.58322851 | 0.065499692 | | |
| | | | | | ZJKN | 0.168458051 | 0.582062357 | 0.09805309 | | |
| G2**3 | CR400BF-G | 576 | 13:41 | BJB-ZJK | BJB | 0.063249488 | 0.576795757 | 0.036482036 | 1.258379380 | 2.184686424 |
| | | | | | QH | 0.328897339 | 0.58383215 | 0.192020841 | | |
| | | | | | BDLX | 0.581895292 | 0.583885792 | 0.339760393 | | |
| | | | | | XBA | 0.733694064 | 0.569474586 | 0.417820123 | | |
| | | | | | XBY | 0.316247442 | 0.580832601 | 0.183686824 | | |
| | | | | | ZJKN | 0.151798772 | 0.583727793 | 0.088609162 | | |
| G2**1 | CR400BF-G | 576 | 14:13 | BJB-QH | BJB | 0.085952736 | 0.58240758 | 0.050059525 | 1.178016830 | 2.045168108 |
| | | | | | QH | 0.103143283 | 0.583859133 | 0.060221148 | | |
| | | | | QH-ZJK | QH | 0.230228547 | 0.583859133 | 0.13442104 | | |
| | | | | | BDLX | 0.529525657 | 0.583893292 | 0.309186479 | | |
| | | | | | XBA | 0.667662785 | 0.567678751 | 0.379017976 | | |
| | | | | | XBY | 0.287785683 | 0.583887307 | 0.168034407 | | |
| | | | | | ZJKN | 0.138137128 | 0.557969149 | 0.077076256 | | |
| G9**1 | CR400BF-G | 576 | 15:38 | BJB-QH | BJB | 0.085952736 | 0.582845688 | 0.050097182 | 1.308649656 | 2.271961208 |
| | | | | | QH | 0.103143283 | 0.583832711 | 0.060218423 | | |
| | | | | QH-BDL | QH | 0.271906488 | 0.583832711 | 0.158747902 | | |

**TABLE 8.** *(Continued.)* **Table of train carbon emissions from 6 AM to 9 PM.**

| | | | | | | | | | | |
|---|---|---|---|---|---|---|---|---|---|---|
| | | | | BDL-DHYB | BDLX | 0.33988311 | 0.583884795 | 0.19845258 | | |
| | | | | | BDLX | 0.28718745 | 0.583884795 | 0.167684386 | | |
| | | | | DHYB-HL | XBA | 0.264347613 | 0.579357389 | 0.153151743 | | |
| | | | | HL-XHB | XBA | 0.410334114 | 0.579357389 | 0.237730101 | | |
| | | | | | XBY | 0.18853189 | 0.583883982 | 0.110080751 | | |
| | | | | XHB-ZJK | XBY | 0.118239628 | 0.583883982 | 0.069038225 | | |
| | | | | | ZJKN | 0.177359442 | 0.583269564 | 0.103448364 | | |
| G2**7 | CR400BF-G | 576 | 16:05 | BJB-QH | BJB | 0.085952736 | 0.559932062 | 0.048127693 | 1.155280726 | 2.005695704 |
| | | | | | QH | 0.103143283 | 0.583840979 | 0.060219275 | | |
| | | | | QH-ZJK | QH | 0.224502158 | 0.583840979 | 0.13107356 | | |
| | | | | | BDLX | 0.516354964 | 0.58388725 | 0.30149308 | | |
| | | | | | XBA | 0.651056259 | 0.581399501 | 0.378523784 | | |
| | | | | | XBY | 0.280627698 | 0.583885247 | 0.163854373 | | |
| | | | | | ZJKN | 0.134701295 | 0.534434071 | 0.071988961 | | |
| G2**5 | CR400BF-G | 0:00 | 17:50 | BJB-ZJK | BJB | 0.062229326 | 0.576795757 | 0.035893611 | 1.238082748 | 2.149449216 |
| | | | | | QH | 0.323592494 | 0.58383215 | 0.188923701 | | |
| | | | | | BDLX | 0.572509797 | 0.583885792 | 0.334280336 | | |
| | | | | | XBA | 0.721860178 | 0.569474586 | 0.411081026 | | |
| | | | | | XBY | 0.311146629 | 0.580832601 | 0.180724106 | | |
| | | | | | ZJKN | 0.149350382 | 0.583727793 | 0.087179969 | | |
| G2**5 | CR400BF-G | 576 | 18:57 | BJB-QH | BJB | 0.085952736 | 0.583233726 | 0.050130534 | 1.181297346 | 2.050863448 |
| | | | | | QH | 0.103143283 | 0.583864387 | 0.06022169 | | |
| | | | | QH-XHB | QH | 0.220444545 | 0.583864387 | 0.128709719 | | |
| | | | | | BDLX | 0.507022454 | 0.583892908 | 0.296046815 | | |
| | | | | | XBA | 0.639289181 | 0.583569603 | 0.373069733 | | |
| | | | | | XBY | 0.187377863 | 0.583889571 | 0.10940798 | | |
| | | | | XHB-ZJK | XBY | 0.112305367 | 0.583889571 | 0.065573933 | | |
| | | | | | ZJKN | 0.168458051 | 0.582560114 | 0.098136941 | | |
| G9**1 | CR400BF-G | 576 | 19:56 | BJB-QH | BJB | 0.085952736 | 0.583759244 | 0.050175704 | 1.238299371 | 2.149825298 |
| | | | | | QH | 0.103143283 | 0.58386028 | 0.060221266 | | |
| | | | | QH-XHYB | QH | 0.276837409 | 0.58386028 | 0.161634367 | | |
| | | | | | BDLX | 0.530605033 | 0.58389292 | 0.309816522 | | |
| | | | | | XBA | 0.507535249 | 0.583543143 | 0.296168715 | | |
| | | | | XHYB-XHB | XBA | 0.124608195 | 0.583543143 | 0.072714258 | | |
| | | | | | XBY | 0.211833932 | 0.58388548 | 0.123686757 | | |
| | | | | XHB-ZJK | XBY | 0.112305367 | 0.583829963 | 0.065567238 | | |
| | | | | | ZJKN | 0.168458051 | 0.583614398 | 0.098314544 | | |
| | CRH5A | 586 | 20:16 | BJB-QH | BJB | 0.085952736 | 0.58387134 | 0.050185339 | 1.482302100 | 2.529525768 |

**TABLE 8.** *(Continued.)* **Table of train carbon emissions from 6 AM to 9 PM.**

| | | | | | |
|---|---|---|---|---|---|
| | | QH | 0.103143283 | 0.583861261 | 0.060221367 |
| | | QH | 0.266608969 | 0.583861261 | 0.155662649 |
| | QH-HL | BDLX | 0.613200629 | 0.583893215 | 0.358043687 |
| | | XBA | 0.279939418 | 0.583393285 | 0.163314776 |
| D***3 | HL-XHYB | XBA | 0.361676427 | 0.583393285 | 0.210999599 |
| | XHYB-XHB | XBA | 0.336442127 | 0.583393285 | 0.196278077 |
| | | XBY | 0.211833932 | 0.583887861 | 0.123687261 |
| | XHB-ZJK | XBY | 0.112305367 | 0.583887861 | 0.065573741 |
| | | ZJKN | 0.168458051 | 0.583739411 | 0.098335604 |

The calculation of carbon emission factors in this paper involves tracing the power supply sources through reverse flow tracking technology. This allows for a precise calculation of carbon emissions from each traction station in different time slots and stations. However, there are still some areas could be improved: first, the current calculation of high-speed trains still relies on average speeds and full seating rates, affecting the accuracy, and further data acquisition and research are needed. Second, research on recommendation methods for low-carbon travel on high-speed rail could be combined with users' travel needs and preferences. Third, with the future construction of new power systems and the increased use of clean energy, carbon emissions from high-speed rail will be further reduced; it is recommended to plan for high-speed rail traction stations to be powered by clean energy during the planning phase.

In summary, the method of calculating carbon emissions from high-speed rail electric traction based on dynamic electricity carbon emission factors provides a scientific basis and decision-making support for environmental assessments and green travel choices of high-speed rail. Future research can further expand, optimize, and apply this method, making a greater contribution to green travel and environmentally friendly transportation.

## APPENDIX A

See Table 8.

## ACKNOWLEDGMENT

The authors would like to extend their deepest appreciation to all those who provided the possibility to complete this research article. Special thanks are reserved for Dr. Li Bingjie, whose expertise and knowledge were invaluable throughout both the research and writing process of this work. Her guidance has been nothing short of inspiring. The research team at the Advanced Research Institute deserves a warm thank you for their camaraderie, technical support, and for fostering an environment conducive to academic exploration. Lastly, they express their utmost respect and heartfelt gratitude to their families and friends, who have shown endless patience and understanding. Their moral support during periods of intense research was a crucial element of the success achieved.

## REFERENCES

[1] "Xi Jinping's speech at the national conference on ecological and environmental protection," (in Chinese), Seeking Truth, no. 22, 2023.
[2] *Our World in Data. Global $CO_2$ Emissions From Fossil Fuels*. Acessed: Mar. 7, 2024. [Online]. Available: https://ourworldindata.org/co2-emissions
[3] P. Friedlingstein et al., "Global carbon budget 2022," *Earth Syst. Sci. Data*, vol. 14, pp. 4811–4900, Nov. 2022.
[4] L. Tan., "Situation requirements and policy priorities of road traffic carbon reduction in China," *China Highway*, vol. 1, no. 3, pp. 88–95, 2023.
[5] Z. Jingyi, "How to be a 'pioneer' in transportation under the goal of 'dual carbon,'" *China Econ. Herald*, p. 2, Jul. 2022.
[6] L. U. Huapu and F. Haixia, "Analysis and consideration of carbon neutrality in transportation," *Economic Guide Sustainable Development*, vol. 1, pp. 63–67, Jun. 2022.
[7] H. Lichen and C. Qiaosong., "Analysis of countermeasures for green development in transportation sector under the goal of carbon neutrality," *Urban Transp.*, vol. 19, no. 5, pp. 36–42, 2021.
[8] M. Liu, J. Wang, J. Wen, G. He, J. Wu, H. Chen, and X. Yang, "Carbon emission levels and intensity analysis of China's transportation industry and different transportation modes," *Prog. Climate Change Res.*, vol. 19, no. 3, pp. 347–347, 2023.
[9] S. Greaves, "Transport energy use and greenhouse gases in urban passenger transport systems: A study of 84 global cities," Associate Professor Sustain. Settlements Inst. Sustainability Technol. Policy, Murdoch Univ., Murdoch, WA, Australia, 2003, no. 2, pp. 87–92.
[10] G. Darido, M. Torres-Montoya, and S. Mehndiratta, "Urban transport and $CO_2$ emissions: Some evidence from Chinese cities," *WIREs Energy Environ.*, vol. 3, no. 2, pp. 122–155, Mar. 2014.
[11] X. Hansheng, H. Yin, and M. Long, "Research on energy conservation and environmental protection effects and benefit analysis of high speed railways," *Environ. Protection Safety Health*, vol. 1, no. 1, pp. 19–22, 2011.
[12] Z. Banruo and L. Zijie., "Can high-speed rail promote a low-carbon economy—Research on the impact and mechanism of high speed rail opening on urban carbon emission intensity," *J. Huazhong Univ. Sci. Technol.*, vol. 35, no. 1, pp. 131–140, 2021.
[13] X. Chao and X. Zhenyu, "The mechanism and effect of high-speed rail opening on urban carbon emissions under the," *J. Changsha Univ. Technol.*, vol. 38, no. 1, pp. 117–130, 2023.
[14] Z. Xinjun, "Does China still need to vigorously develop high speed rail—Also discussing the energy conservation and emission reduction effects of high speed rail," *China Econ. Rep.*, vol. 1, no. 7, pp. 66–69, 2015.
[15] F. Yanbing, L. Hengbin, and Z. Sufen., "Calculation method for carbon emissions during the lifecycle of high-speed railways," *China Railway Sci.*, vol. 34, no. 5, pp. 140–144, 2013.
[16] M. Chester and A. Horvath, "Life-cycle assessment of high-speed rail: The case of California," *Environ. Res. Lett.*, vol. 5, no. 1, pp. 1–8, 2010.
[17] R. Damián and C. I. Zamorano, "Life cycle greenhouse gases emissions from high-speed rail in spain: The case of the Madrid—Toledo line," *Sci. Total Environ.*, vol. 901, Nov. 2023, Art. no. 166543.

[18] J. Chen, X. Wang, X. Wang, X. Ma, and Y. Chen, "Calculation of carbon emissions throughout the entire lifecycle of high-speed railways," *J. Railways*, vol. 38, no. 12, pp. 47–55, Dec. 2016.
[19] S. Kaewunruen, J. Sresakoolchai, and J. Peng, "Life cycle cost, energy and carbon assessments of Beijing-Shanghai high-speed railway," *Sustainability*, vol. 12, no. 1, p. 206, Dec. 2019.
[20] W. Tiecheng, "Research on the calculation method of energy consumption for high-speed train operation," *Railway Transp. Economy*, vol. 1, no. 34, pp. 88–92, May 2012.
[21] C. Tao, *Calculation Method of Energy Consumption of High-Speed Trains and Quantitative Analysis of its Influencing Factors*. Beijing, China: Beijing Jiaotong University, 2011.
[22] M. Weiwu and L. Liqing, "Energy consumption measurement and evaluation of high-speed trains," Central South Univ. Press, Changsha, China, 2015.
[23] "Methodology for calculating transport emissions and energy consumption," Eur. Commission, Luxembourg, 1999.
[24] N. F. F. Yaacob, M. R. Mat Yazid, K. N. Abdul Maulud, and N. E. Ahmad Basri, "A review of the measurement method, analysis and implementation policy of carbon dioxide emission from transportation," *Sustainability*, vol. 12, no. 14, p. 5873, Jul. 2020.
[25] C. Yuan, S. Zhang, P. Jiao, and D. Wu, "Study on spatiotemporal changes and influencing factors of total factor carbon emissions efficiency in provincial transportation in China," *Resour. Sci.*, vol. 39, no. 4, pp. 687–697, 2017.
[26] Z. Tianrui, "Preliminary theoretical investigation on power system carbon emission flow," *Automat. Electr. Power Syst.*, vol. 36, no. 7, pp. 38–43, 2012.
[27] K. Chongqing, "Recursive calculation method of carbon emission flow in power systems," *Automat. Electr. Power Syst.*, vol. 41, no. 18, pp. 10–16, 2017.
[28] L. Yehui, "Distributed carbon meter system based on carbon emission flow iterative algorithm (Part 1): Theoretical methods and analysis," *Grid Technol.*, vol. 47, no. 6, pp. 2165–2174, 2023.
[29] G. J. Miller, K. Novan, and A. Jenn, "Hourly accounting of carbon emissions from electricity consumption," *Environ. Res. Lett.*, vol. 17, no. 4, Apr. 2022, Art. no. 044073.
[30] T. Zhou, C. Kang, Q. Xu, and Q. Chen, "Preliminary investigation on a method for carbon emission flow calculation of power system," *Automat. Electr. Power Syst.*, vol. 36, no. 11, pp. 44–49, Nov. 2012.
[31] Z. Tianrui et al., "Analysis on distribution characteristics and mechanisms of carbon emission flow in electric power network," *Automat. Electr. Power Syst.*, vol. 36, no. 15, pp. 39–44, 2012.
[32] *Intergovernmental Panel on Climate Change (IPCC)*, United Nations (UN), New York, NY, USA, 2014.
[33] (2022). *China Power Grid Baseline Emission Factors*. [Online]. Available: https://www.mee.gov.cn/xxgk2018/xxgk/xxgk03/202303/W020230315687660073734.pdf
[34] M. Cuimei, L. Shicheng, and G. Quansheng, "Greenhouse gas emission factors for grid electricity for Chinese provinces," *Resour. Sci.*, vol. 1, no. 5, pp. 1005–1012, 2014.
[35] C. Wang, Y. Miao, Y. Wu, Y. Ji, and H. Xu, "Research on carbon reduction and economic environment mutual feedback in China's high speed railway operation," *China Population Resour. Environ.*, vol. 27, no. 9, pp. 171–177, Sep. 2017.

**SONG JINWEI** was born in 1983. He received the bachelor's and master's degrees from China Agricultural University, in 2006 and 2009, respectively, and the Ph.D. degree from the University of Chinese Academy of Sciences, in 2014. He is currently with the Big Data Center of State Grid Corporation of China, where he engages in research related to electric power big data and artificial intelligence. Recently, his focus has been on the application research of electric power data in the field of carbon emission accounting.

**CHEN XIANG** was born in 1985. He received the master's degree from Sichuan University. He is currently with the Big Data Center of State Grid Corporation of China, where he is engaged in research and management in the field of electric power big data and artificial intelligence. Recently, he has been focusing on the application research of electric power data in the field of carbon emission accounting.

**LU CAIXIA** was born in Rizhao, Shandong, in November 1978. She received the master's degree in electric power systems and automation from the Electric Power Research Institute, Beijing, China, in 2003. She is currently working as a Director of Data Application Business Department in Beijing Guodiantong Network Technology Company Ltd. She is mainly engaged in the research of artificial intelligence, large language model, and big data analysis and application.

**SHI XIN** was born in 1991. She received the bachelor's degree from Xi'an Jiaotong University, in 2014, and the Ph.D. degree from the Electric Power Research Institute of China, in 2020. She is currently with the Big Data Center of State Grid Corporation of China, focusing on research in power systems and electric power big data. Recently, her research has been centered on the application of electric power big data in energy consumption and carbon emission fields.

**YAN YUE** was born in 1994. He received the master's degree from Johns Hopkins University, USA, in 2017. He is currently with the Big Data Center of State Grid Corporation of China, primarily working in the fields of the electricity market, power sector carbon emission accounting, energy big data applications, and carbon asset management.

**ZHANG SHIZE** was born in 1994. He received the master's degree from the University of Chinese Academy of Sciences, in 2022. He is currently with the Big Data Center of State Grid Corporation of China, focusing on research in the fields of electric power big data and artificial intelligence. Recently, his research has been centered on the application of power carbon emission factors and related areas.